

Hadron Form Factors

Rolf Ent
Jefferson Lab

Science & Technology Review
July 2002

- Introduction
- Pion Form Factor
- G_E^p/G_M^p ratio
- G_E^n
- G_M^n
- Strangeness Form Factors
- Outlook

How are the Nucleons Made from Quarks and Gluons?

Why are nucleons interacting via V_{NN} such a good approximation to nature?

How do we understand QCD in the confinement regime?

- A) The distribution of u, d, and s quarks in the hadrons
(spatial structure of charge and magnetization in the nucleons is an essential ingredient for conventional nuclear physics; the flavor decomposition of these form factors will provide new insights and a stringent testing ground for QCD-based theories of the nucleon)
- B) The excited state structure of the hadrons
- C) The spin structure of the hadrons
- D) Other hadron properties
(polarizability, quark correlations,)

Nucleon and Pion Form Factors

- Fundamental ingredients in “Classical” nuclear theory
- A testing ground for theories constructing nucleons from quarks and gluons.
 - spatial distribution of charge, magnetization
- Experimental insights into nucleon structure from the flavor decomposition of the nucleon form factors

PRECISION

$$\left. \begin{array}{ccc} G_E^p & G_E^n & G_E^{p,Z} \\ G_M^p & G_M^n & G_M^{p,Z} \end{array} \right\} \Rightarrow \begin{array}{ccc} G_E^u & G_E^d & G_E^s \\ G_M^u & G_M^d & G_M^s \end{array}$$

- Additional insights from the measurement of the form factors of nucleons embedded in the nuclear medium
 - implications for binding, equation of state, EMC...
 - precursor to QGP

Historical Overview

Stern (1932) measured the proton magnetic moment $\mu_p = 2.79 \mu_{\text{Dirac}}$ indicating that the proton was not a point-like particle

Hofstadter (1950's) provided the first measurement of the proton's radius through elastic electron scattering

Subsequent data (≤ 1993) were based on:

- Rosenbluth separation for proton, severely limiting the accuracy for G_E^p at $Q^2 > 1 \text{ GeV}^2$

As yet, no "ab initio" calculations available, waiting for Lattice QCD
Main interpretation based on Vector-Meson Dominance

- In simplest form resulting in dipole form factor:

$$G_D = \left\{ \frac{\Lambda^2}{\Lambda^2 + Q^2} \right\}^2 \quad \text{with } \Lambda = 0.84 \text{ GeV}$$

Adylov et al. (1970's) provided the first measurement of the pion's radius through pion-atomic electron scattering.

Subsequent measurements at Fermilab and CERN (1980's)

"Ab initio" calculations of the pion far simpler

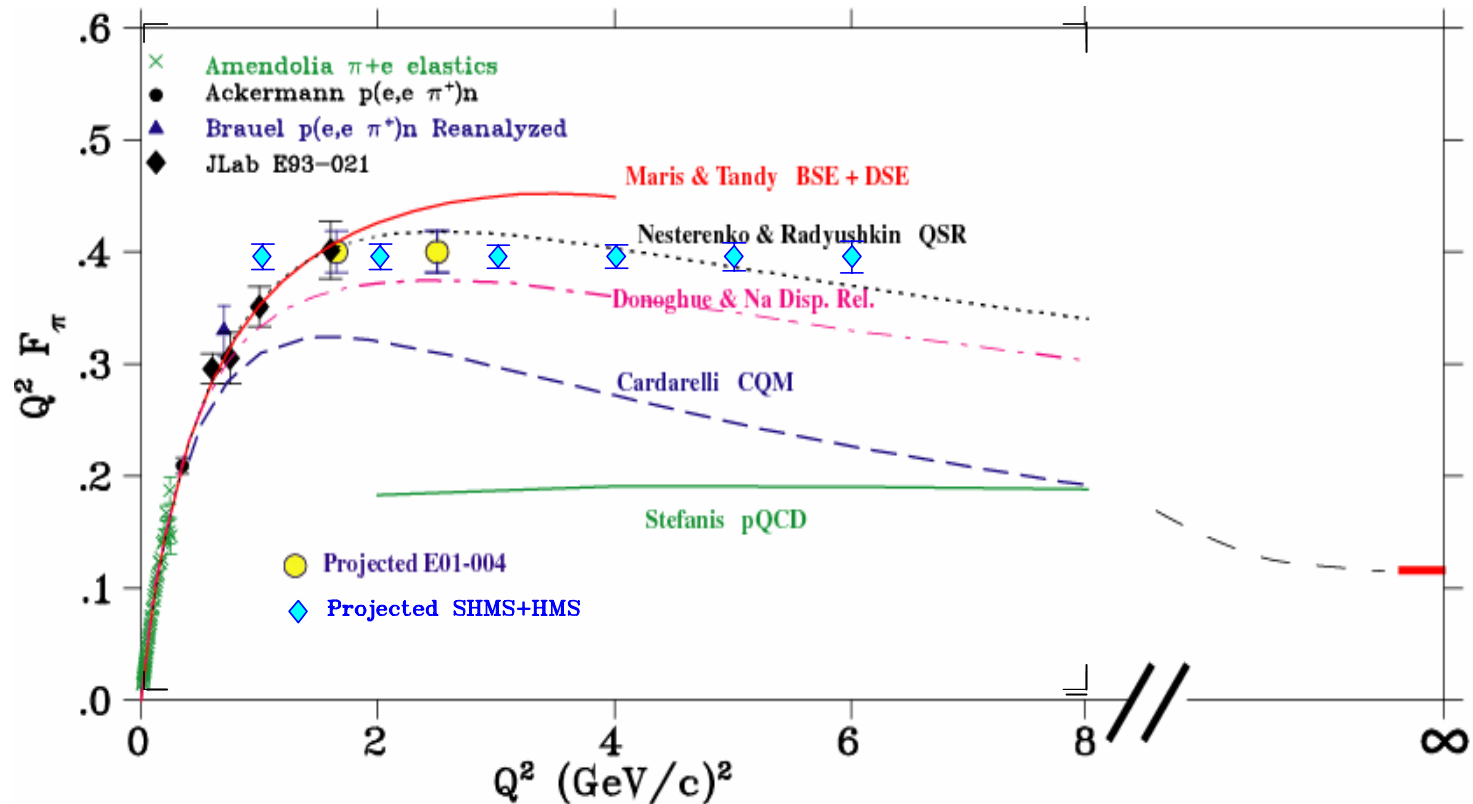
- In asymptotic region, $F_\pi \rightarrow 8\pi\alpha_s f_\pi^2 Q^{-2}$

Proton

Pion

Charged Pion Electromagnetic Form Factor

Potential to approach region where perturbative QCD applies



Hall C E93-021 results

Projected E01-004 and 12 GeV results

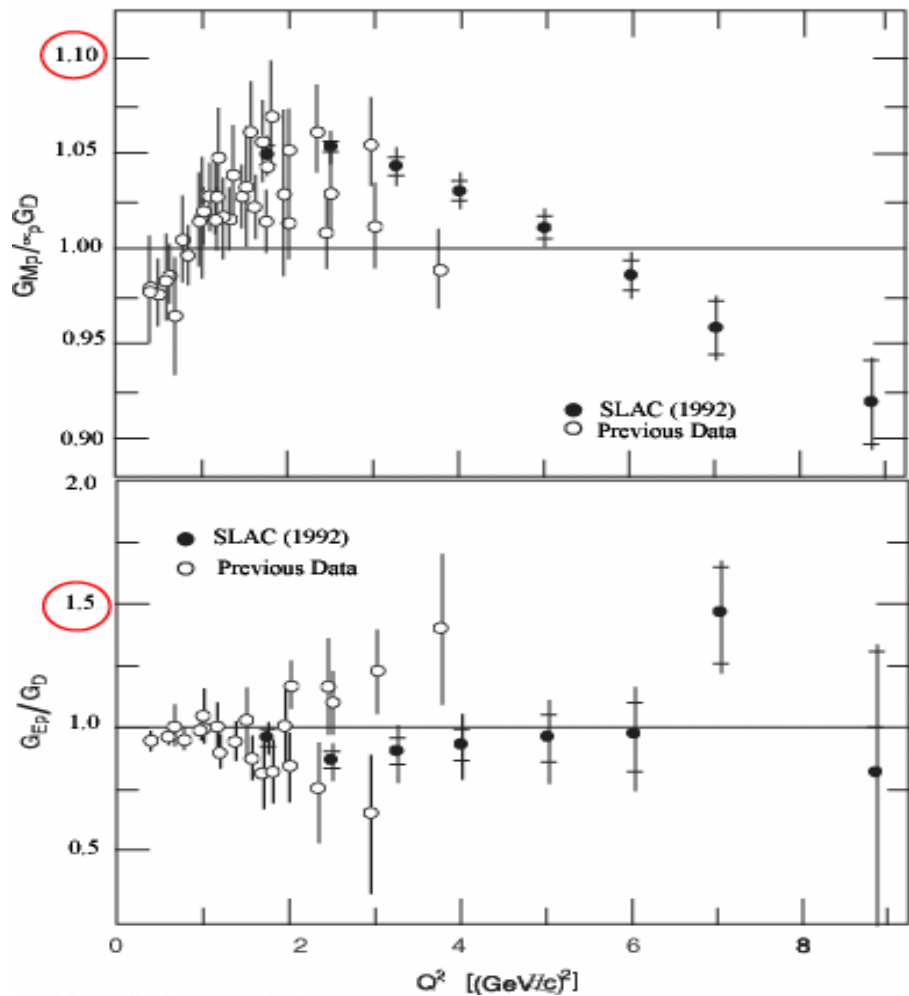


◆ Projected SHMS+HMS



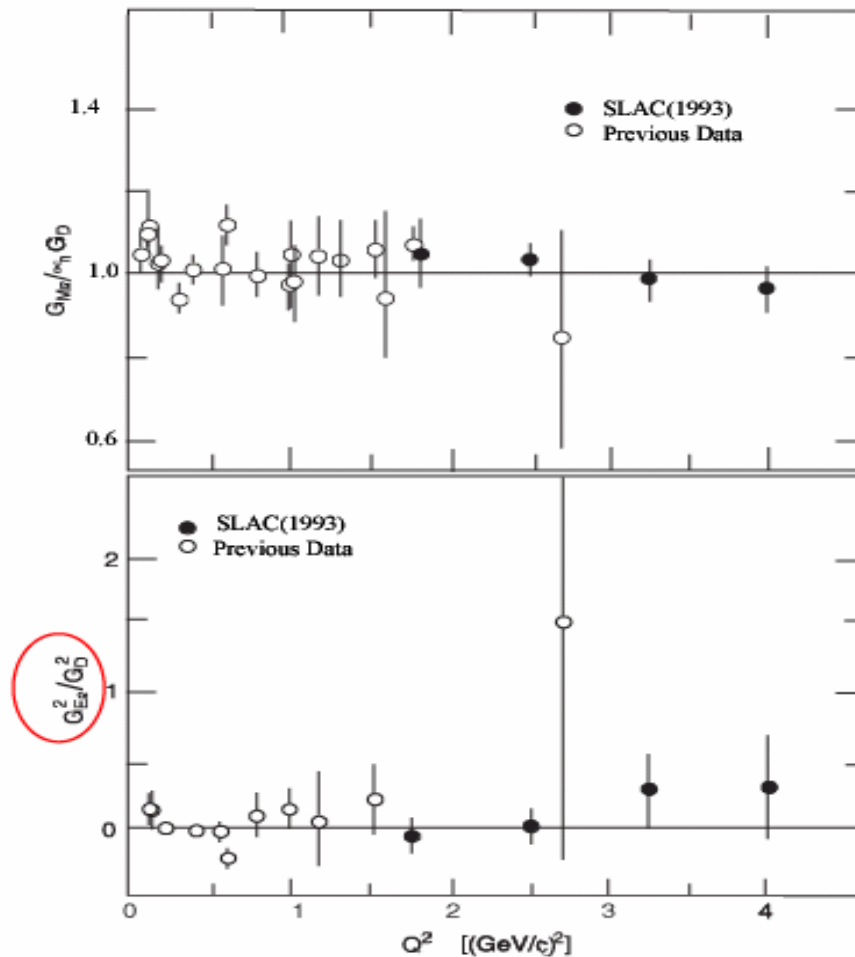
World Data in 1993

Proton



VMD models

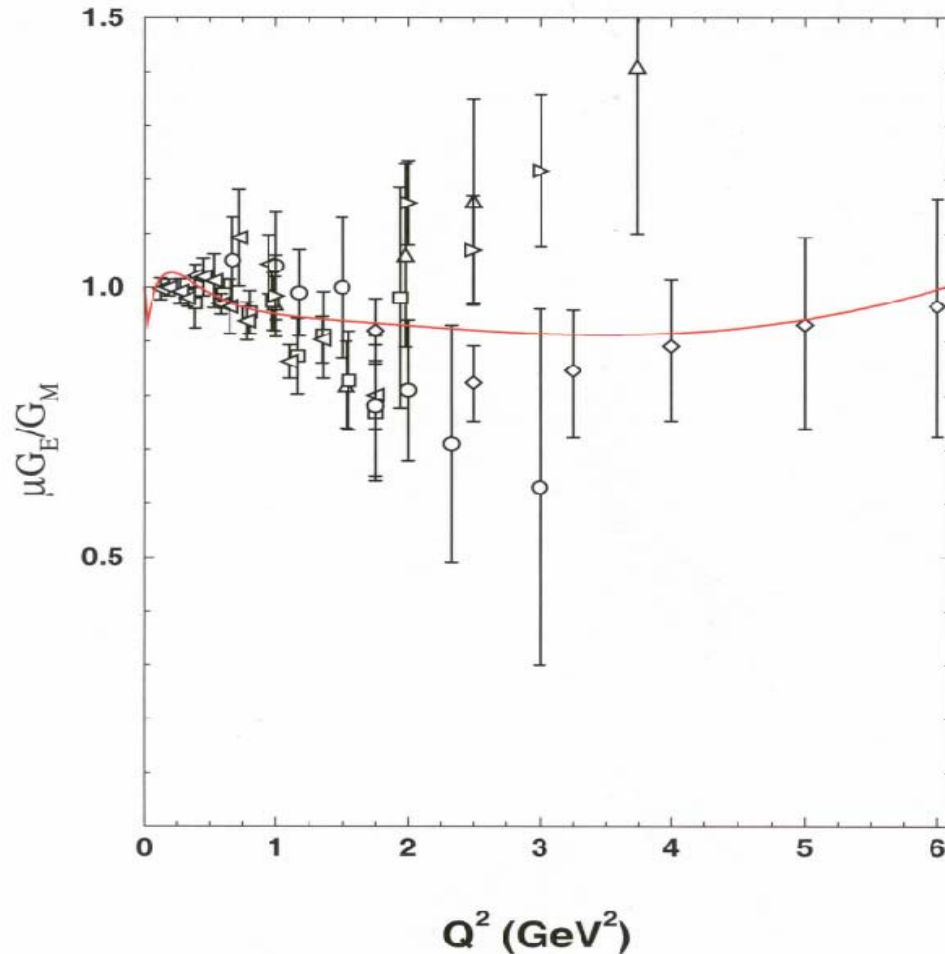
Neutron



Measurement of G_E^p/G_M^p to $Q^2 = 5.6 \text{ GeV}^2$ (E99-007)

Earlier nucleon form factor data used Rosenbluth separation

Leading to large systematic errors in G_E^p since $G_E^p < G_M^p$ for $Q^2 > 1 \text{ (GeV/c)}^2$



— Best fit

Measurement of G_E^p/G_M^p to $Q^2 = 5.6 \text{ GeV}^2$ (E99-007)

Earlier nucleon form factor data used Rosenbluth separation
Leading to large systematic errors in G_E^p since $G_E^p < G_M^p$ for $Q^2 > 1 \text{ (GeV/c)}^2$

Polarization observables resolve this shortcoming
f.i. by measuring recoil polarization:

$$^1\text{H}(\vec{e}, e' \vec{p})$$

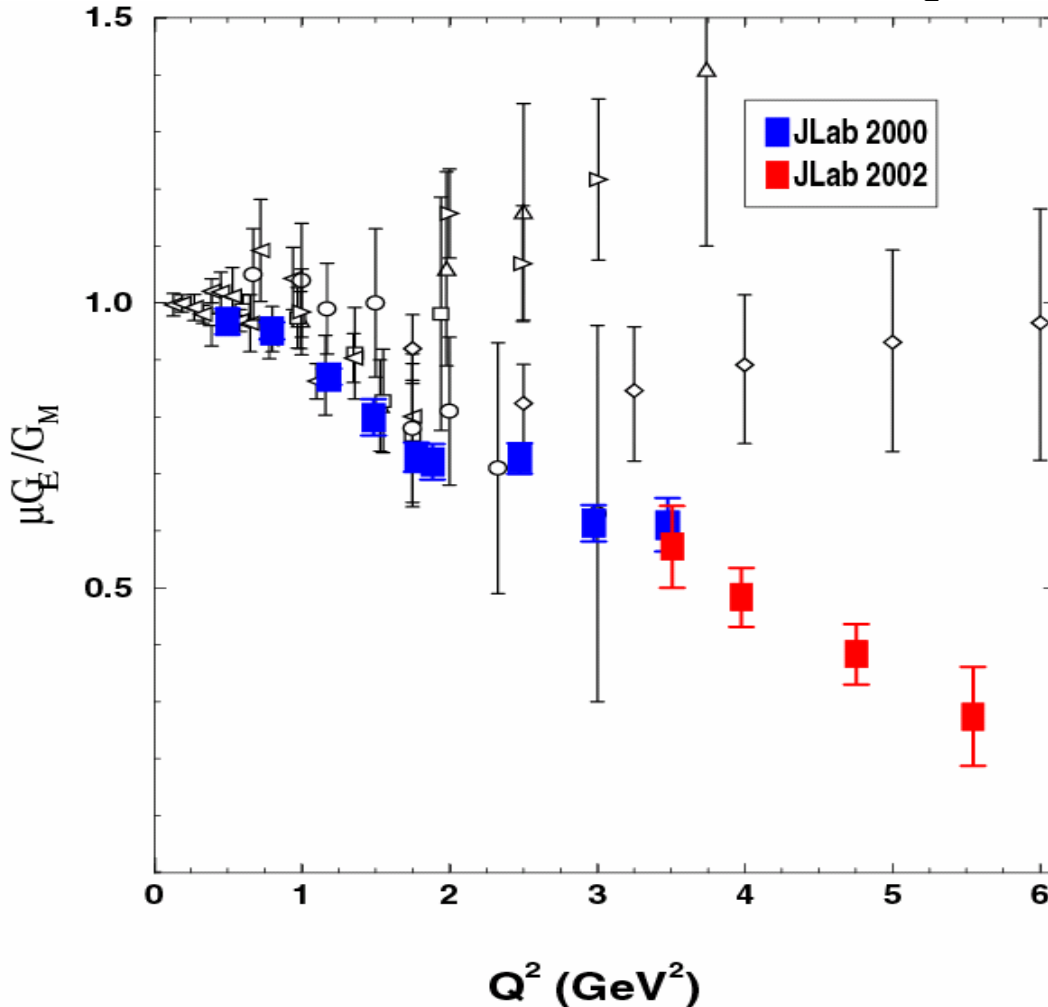
$$\frac{G_E^p}{G_M^p} = -\frac{P_t}{P_l} \frac{E_e + E_{e'}}{2M} \tan\left(\frac{\theta_e}{2}\right)$$

Key is high beam current
high polarization
focal plane polarimeter

Measurement of G_E^p/G_M^p to $Q^2 = 5.6 \text{ GeV}^2$ (E99-007)

Earlier nucleon form factor data used Rosenbluth separation

Leading to large systematic errors in G_E^p since $G_E^p < G_M^p$ for $Q^2 > 1 \text{ (GeV/c)}^2$



E93-027 observed linear decrease of G_E^p/G_M^p

E99-007 extended the data set to 5.6 (GeV/c)^2 using a Pb-glass calorimeter

Linear trend is observed to continue

The data do not approach basic pQCD scaling

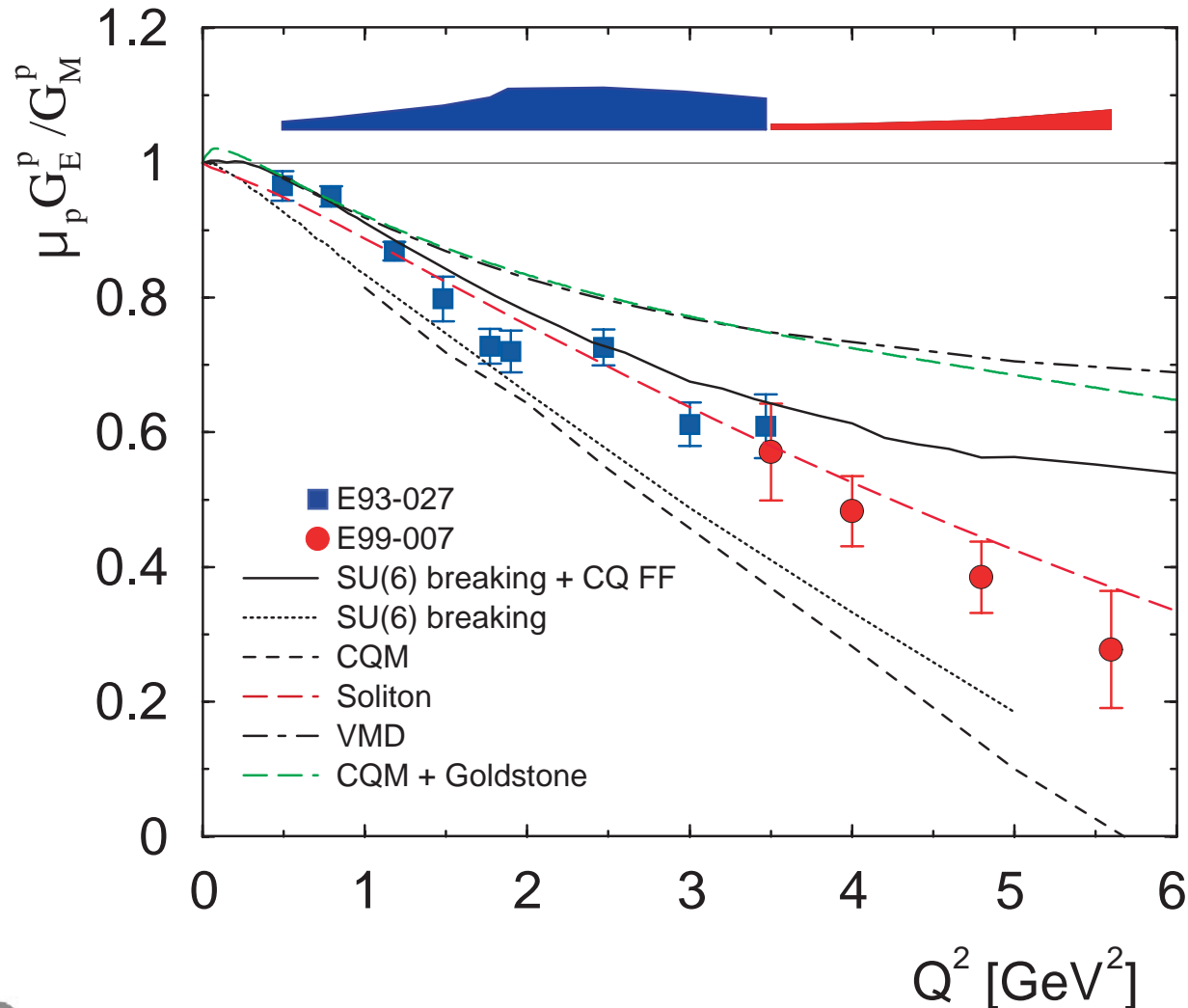
$$F_2/F_1 \propto 1/Q^2 \text{ (Björken)}$$

Ralston et al. include quark orbital angular momentum L_q

$$\boxtimes F_2/F_1 \propto 1/Q$$

Measurement of G_E^p/G_M^p to $Q^2=5.6 \text{ GeV}^2$

Hall A E93-027 and E99-007 results



Radial Charge Distribution

In Breit frame

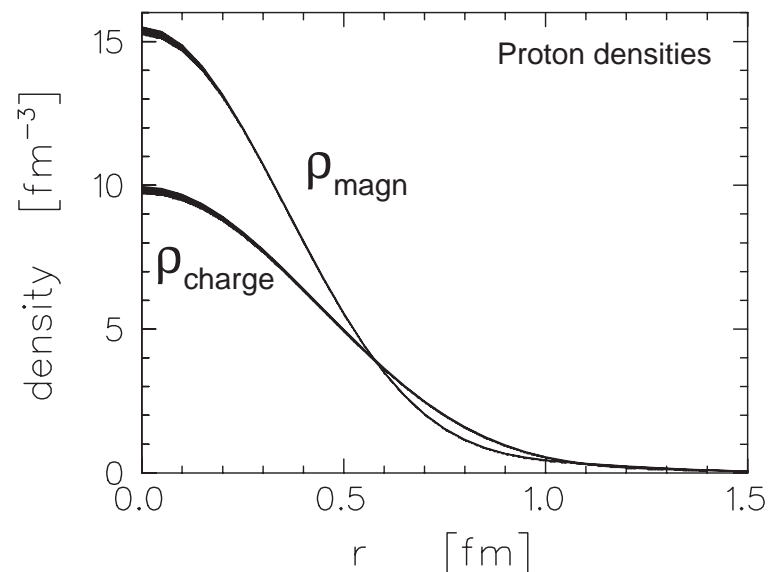
$$G_E^p(k^2) = \int p(r) j_0(kr) r^2 dr \text{ with } k^2 = \frac{Q^2}{1 + \tau}$$

k first-order correction for Breit-frame transformation

• Fourier-Bessel analysis

$$\rho(r) = \sum_{n=1}^{n=n_{\max}} a_n j_0(k_n r) \Theta(R - r) \text{ with } k_n = n\pi / R$$

Jim Kelly



Extensions

J. Arrington and R. Segel

E01-001 (Hall A)

Super Rosenbluth separation

$$R_1 = \frac{\sigma(E_A, Q_1^2)}{\sigma(E_B, Q_1^2)} = K_1 \frac{\rho_1^2 + \varepsilon_{A1}^{-1} K Q_1^2}{\rho_1^2 + \varepsilon_{B1}^{-1} K Q_1^2}$$

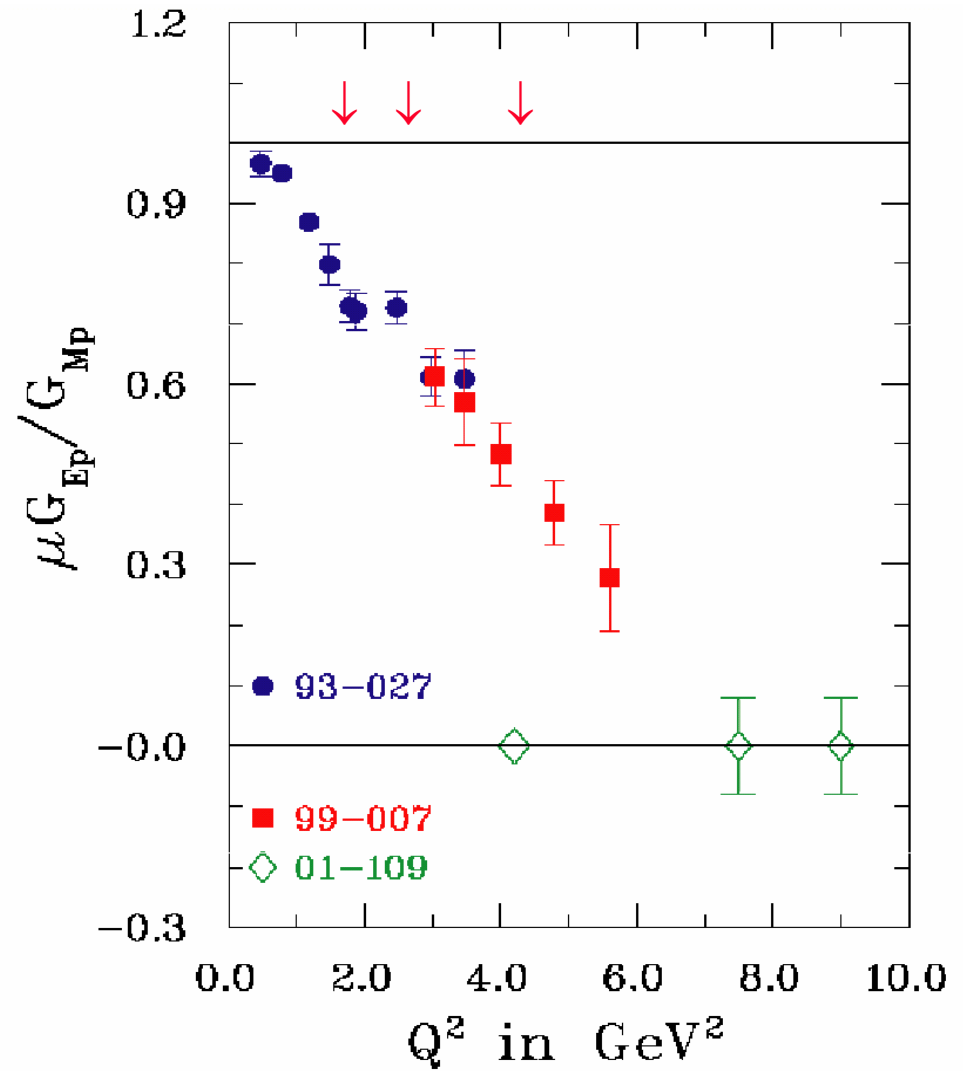
with $\rho_1 = \frac{G_E^P}{G_M^P}$

at $Q_1^2=1.9, 2.8$ and 4.2 GeV^2
and $Q_2^2=0.5 \text{ GeV}^2$

C.F. Perdrisat *et al.*

E01-109 (Hall C)

Use HMS (with new Focal Plane
Polarimeter)
and larger Pb-glass calorimeter

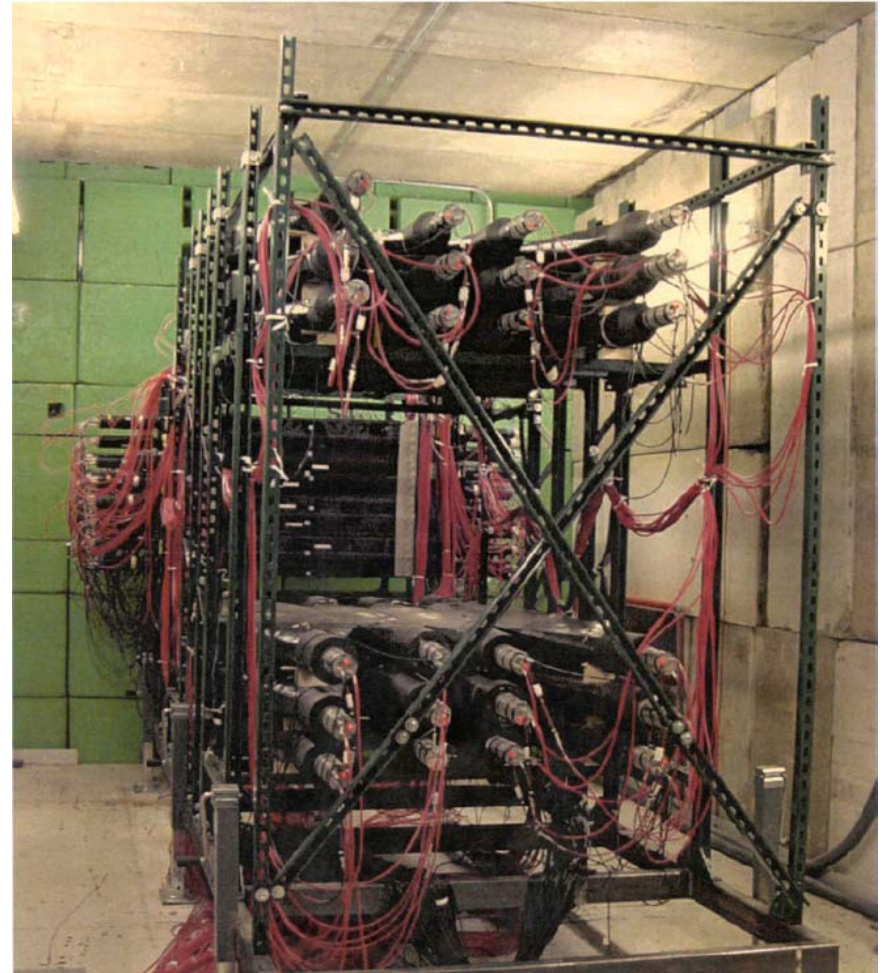
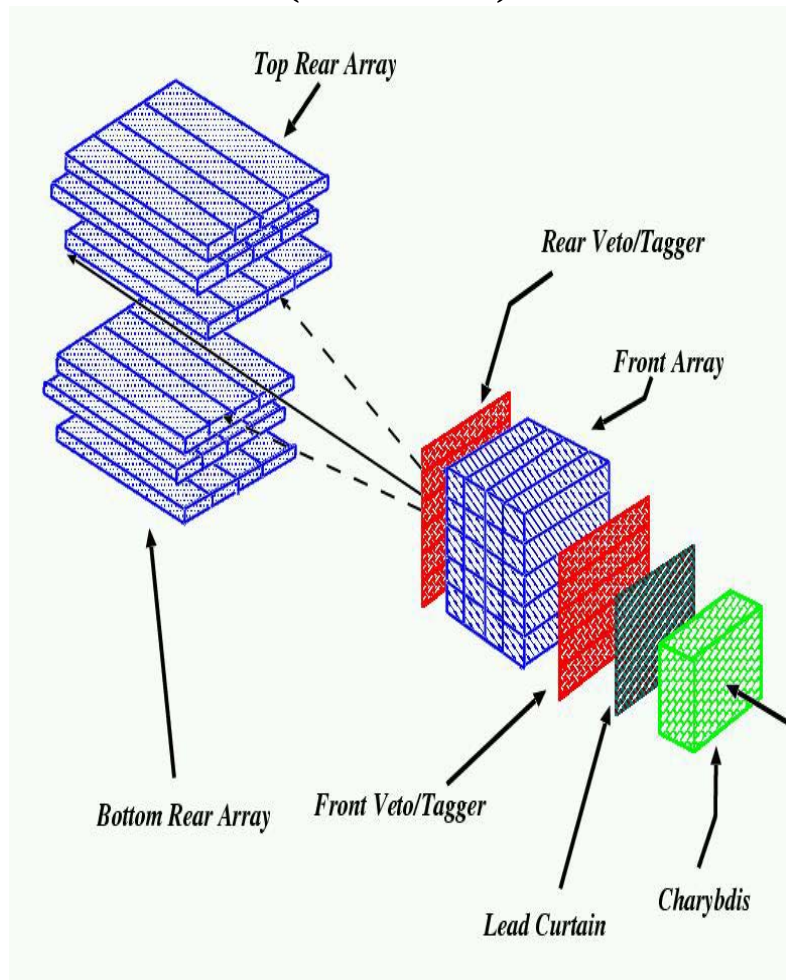


gpp he 007 rll 11/20/01

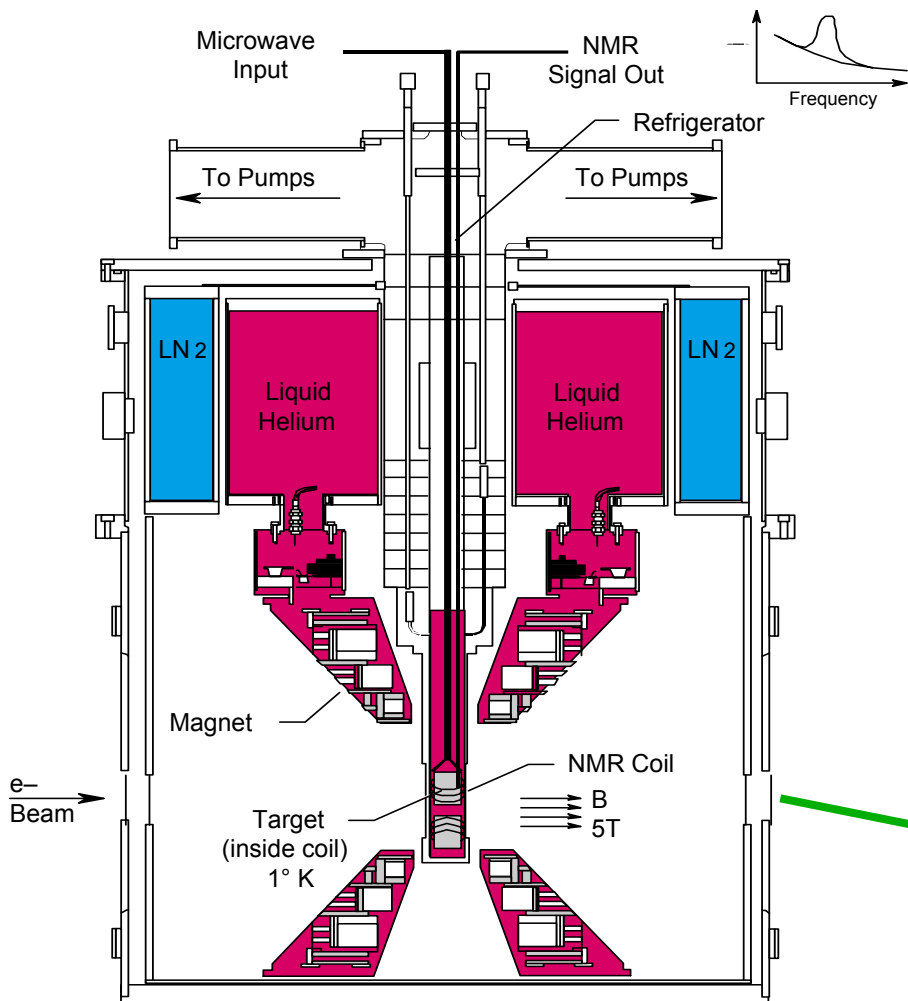


G_E^n Experiment with Neutron Polarimeter

$$^2H(\vec{e}, e' \vec{n})$$

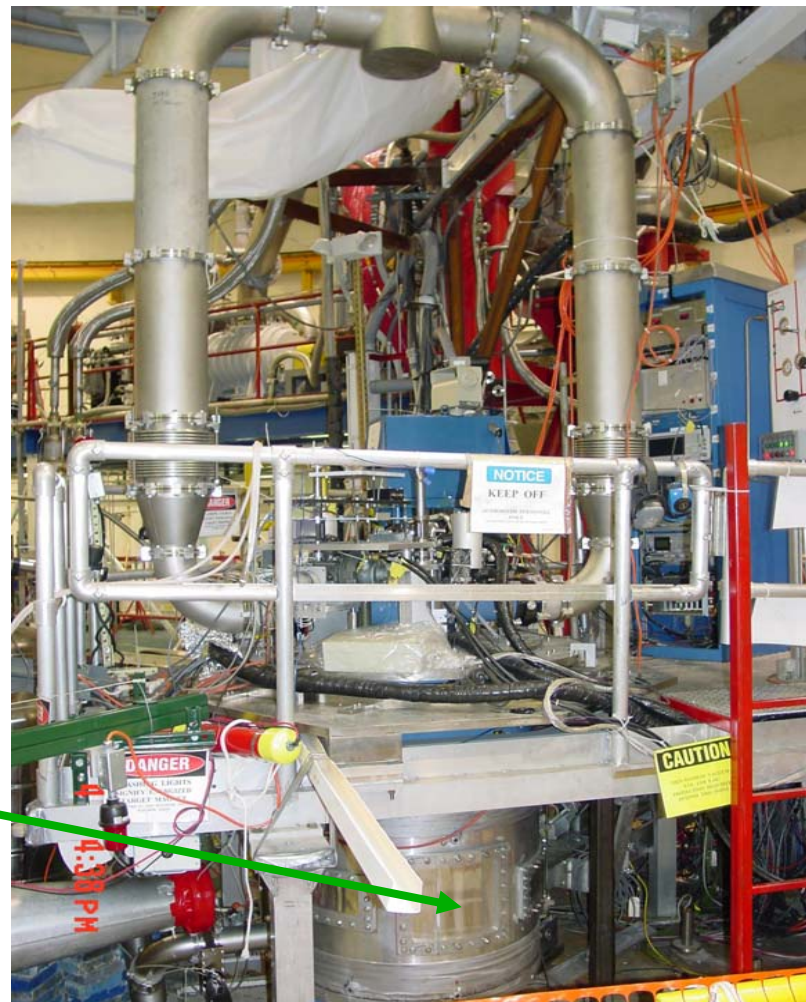


G^n_E Experiment with DNP ND_3 Target $^2\vec{H}(\vec{e}, e'n)$



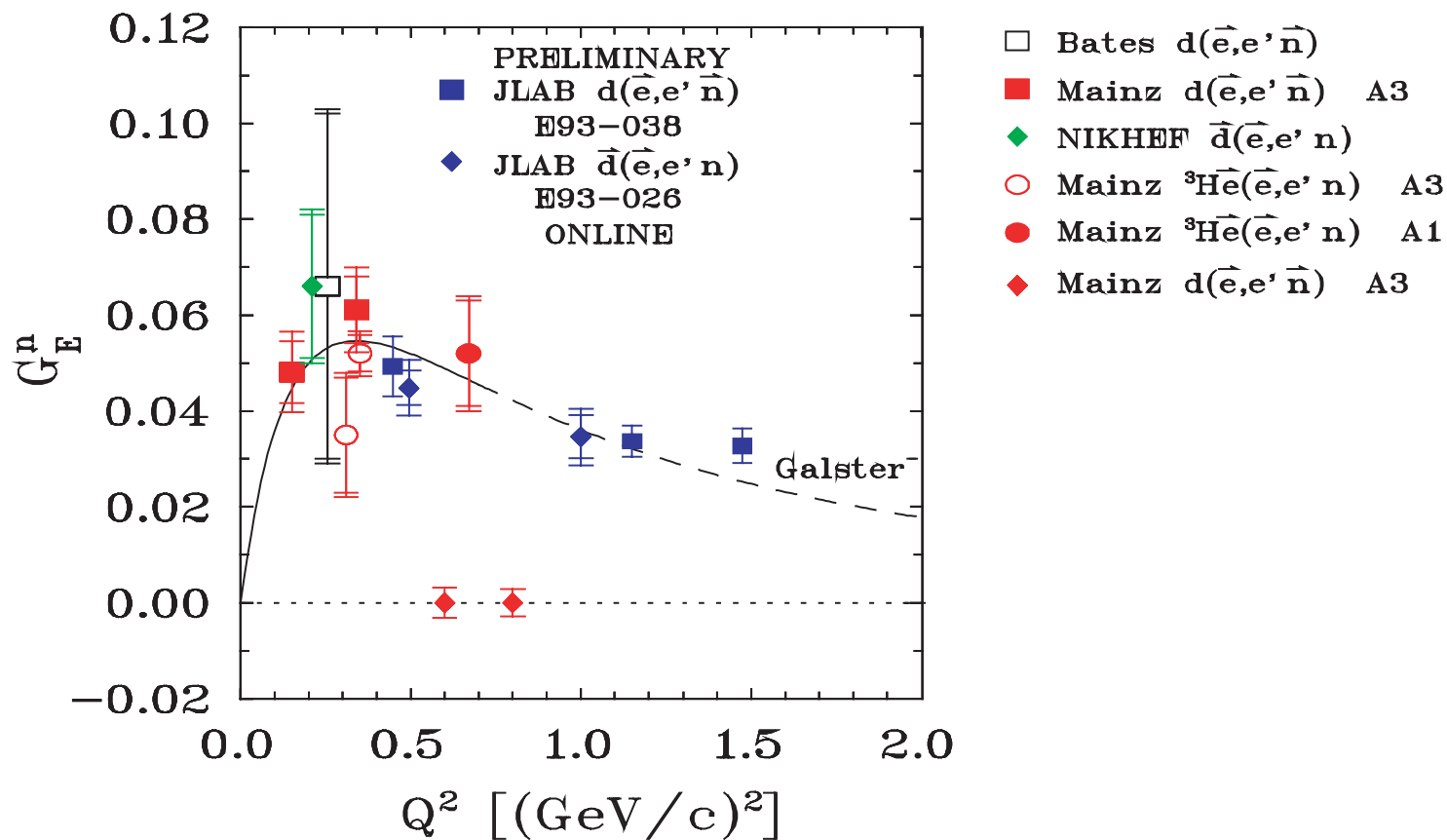
4-94

7656A1



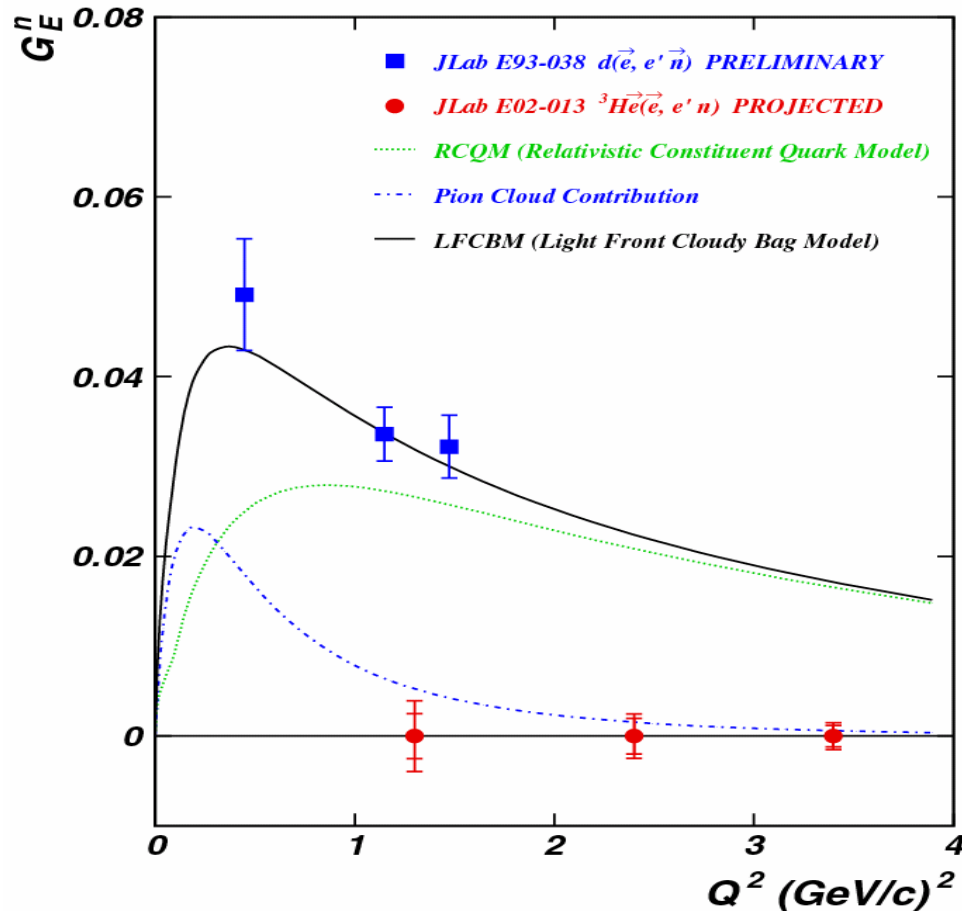
Neutron Electric Form Factor G_E^n

- G_E^n (Madey, Kowalski) – high current polarized beam, unpolarized LD_2 target, neutron polarimeter & neutron precession magnet.
- G_E^n (Day) – low intensity polarized beam ND_3 polarized target and neutron detector.



Neutron Electric Form Factor G_E^n

Hall C Experiment E93-038 (Madey, Kowalski)



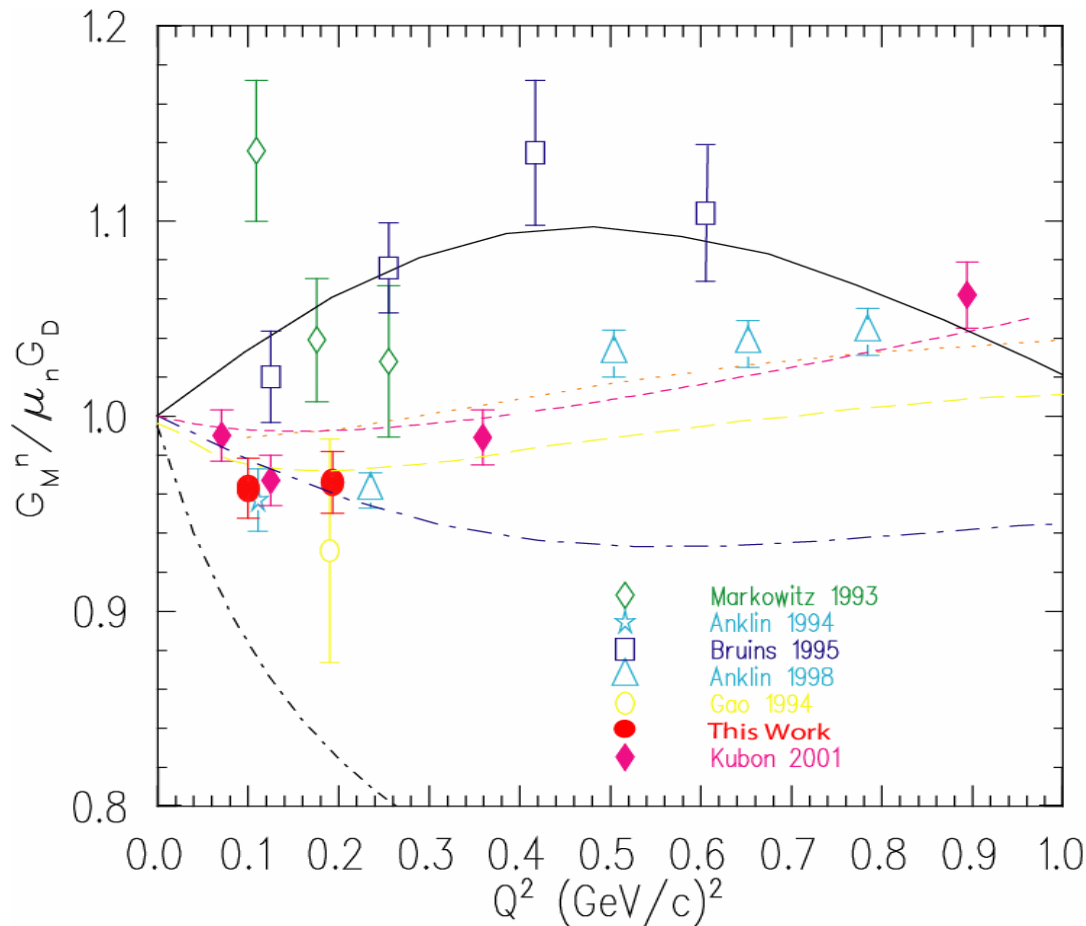
Pion cloud
not sufficient

Relativistic effects
important ingredient

- G_E^n (Hall A) – polarized beam, polarized ${}^3\text{He}$ target, and neutron detector

Measurement of G_M^n at low Q^2 from ${}^3\vec{\text{H}}e(\vec{e},e')$

Hall A E95-001

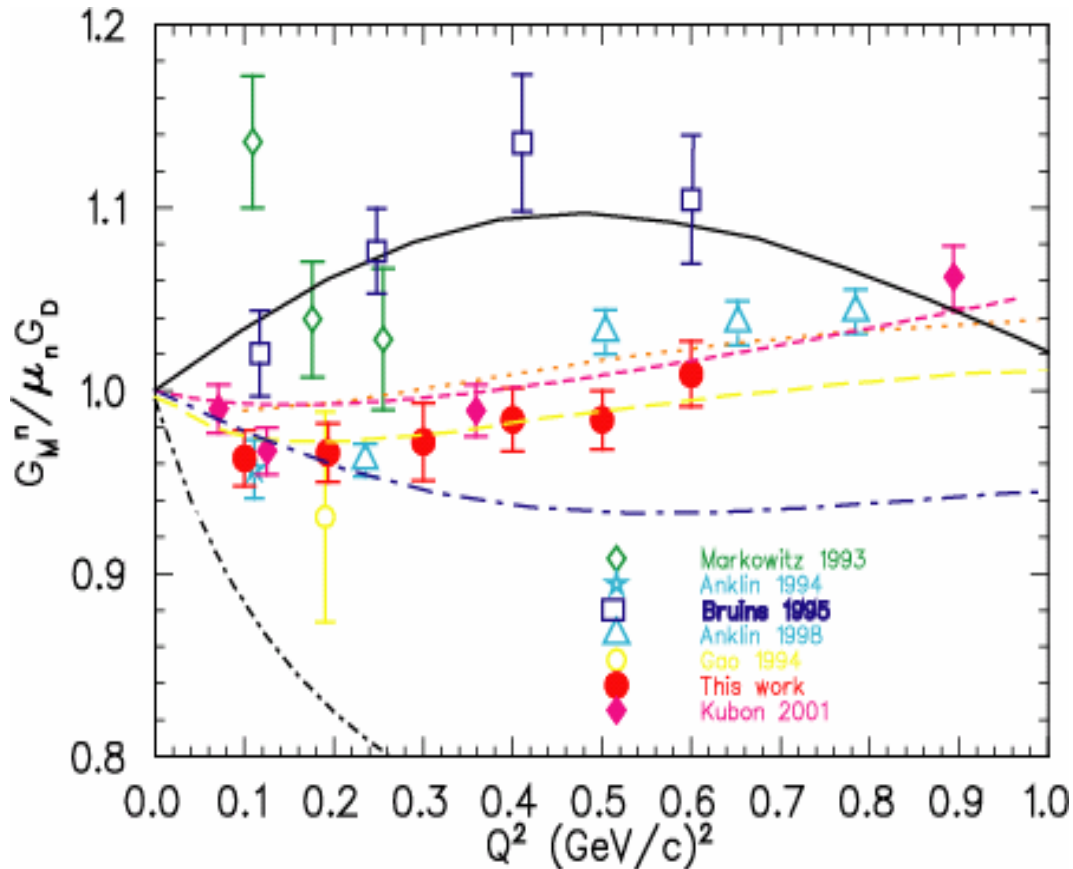


$Q^2=0.1,0.2$ (GeV/c)²
extracted from full
calculation (W.Xu et al.
PRL 85, 2900 (2000))

$Q^2=0.3-0.6$ extracted from
PWIA, more reliable
extraction requires
improved theory (in
progress)

Measurement of G_M^n at low Q^2 from ${}^3\bar{\text{H}}e(\vec{e},e')$

Hall A E95-001

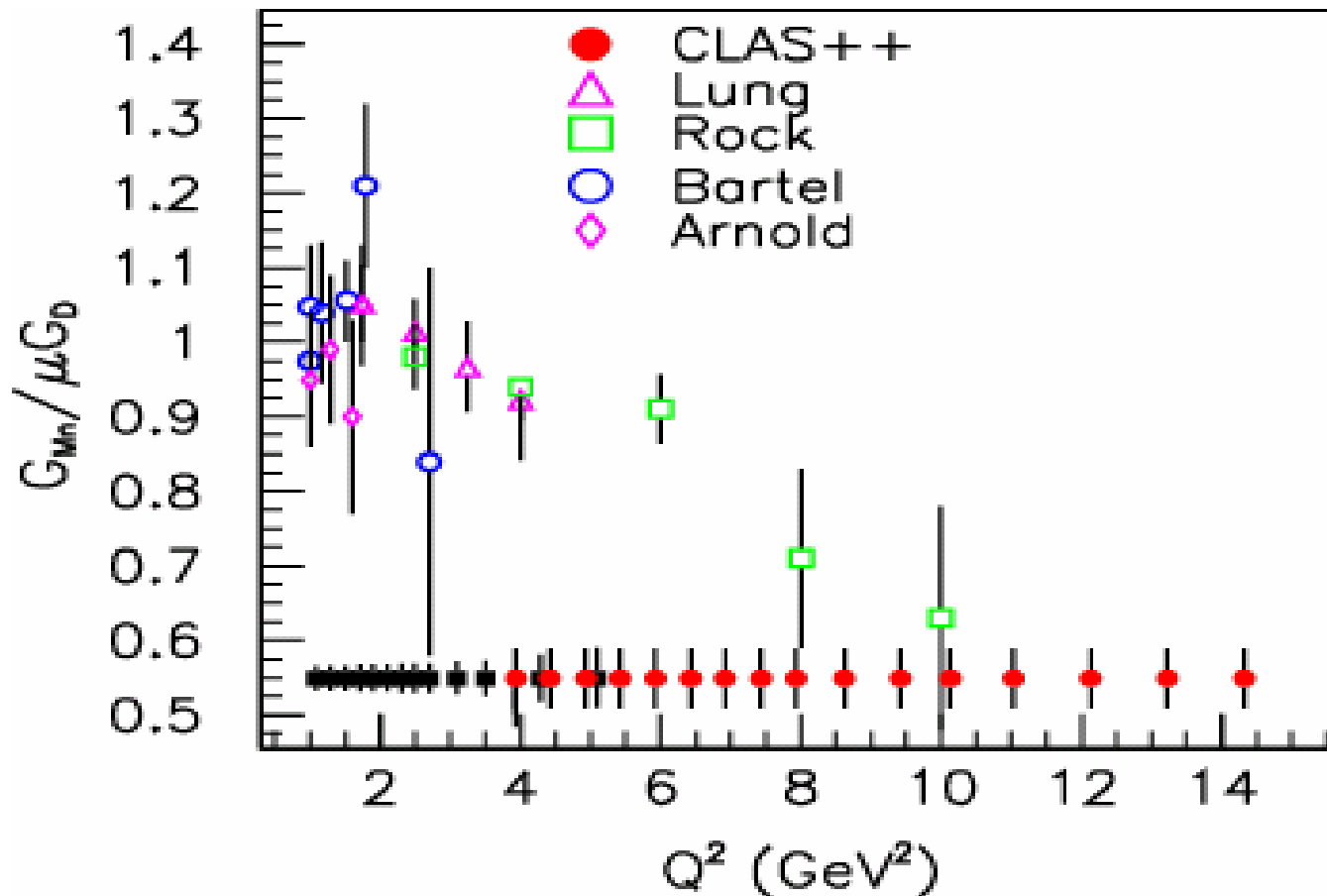


$Q^2=0.1,0.2$ (GeV/c)²
extracted from full
calculation (W.Xu et al.
PRL 85, 2900 (2000))

$Q^2=0.3-0.6$ extracted from
PWIA, more reliable
extraction requires
improved theory (in
progress)

Measurement of G_M^n from CLAS

$$^2\text{H}(e, e'n) / ^2\text{H}(e, e'p) \Rightarrow G_M^n$$



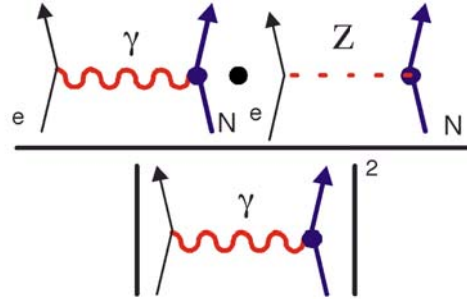
• 6 GeV Projections

• 12 GeV Projections

Strange Quark Currents in the Nucleon G_E^S, G_M^S

Polarized Electron
Unpolarized Target

$$A = \frac{\sigma_R - \sigma_L}{\sigma_R + \sigma_L}$$



For a Nucleon:

$$A = \left[\frac{-G_F Q^2}{4\pi\alpha\sqrt{2}} \right] \frac{\epsilon G_E^\gamma G_E^Z + \tau G_M^\gamma G_M^Z - (1 - 4\sin^2\theta_W)\epsilon' G_M^\gamma G_A^e}{\epsilon (G_E^\gamma)^2 + \tau (G_M^\gamma)^2}$$

forward angles
HAPPEX, Mainz, G^0 : sensitive to

$$G_E^S \text{ and } G_M^S$$

backward angles
SAMPLE, G^0 : sensitive to

$$G_M^S \text{ and } G_A^e$$

weak charge
of the proton

$$Q_{\text{weak}}^p$$

$$\epsilon = 1 / [1 + 2(1 + \tau) \tan^2 \theta/2]$$

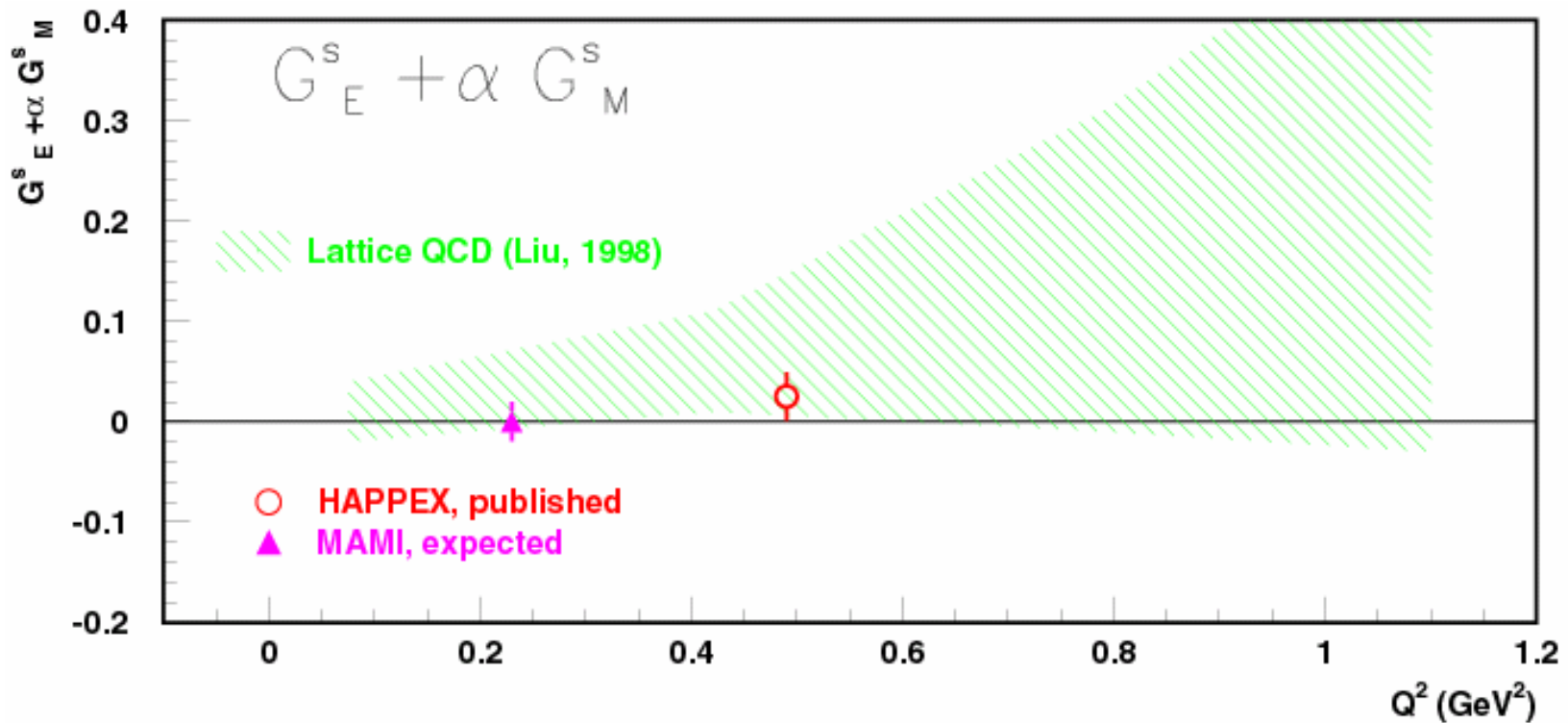
$$\epsilon' = [\tau (1 + \tau)(1 - \epsilon^2)]^{-1/2}$$

$$\tau = Q^2/4m^2$$

Q^2 is the four momentum transfer

θ is the laboratory electron scattering angle

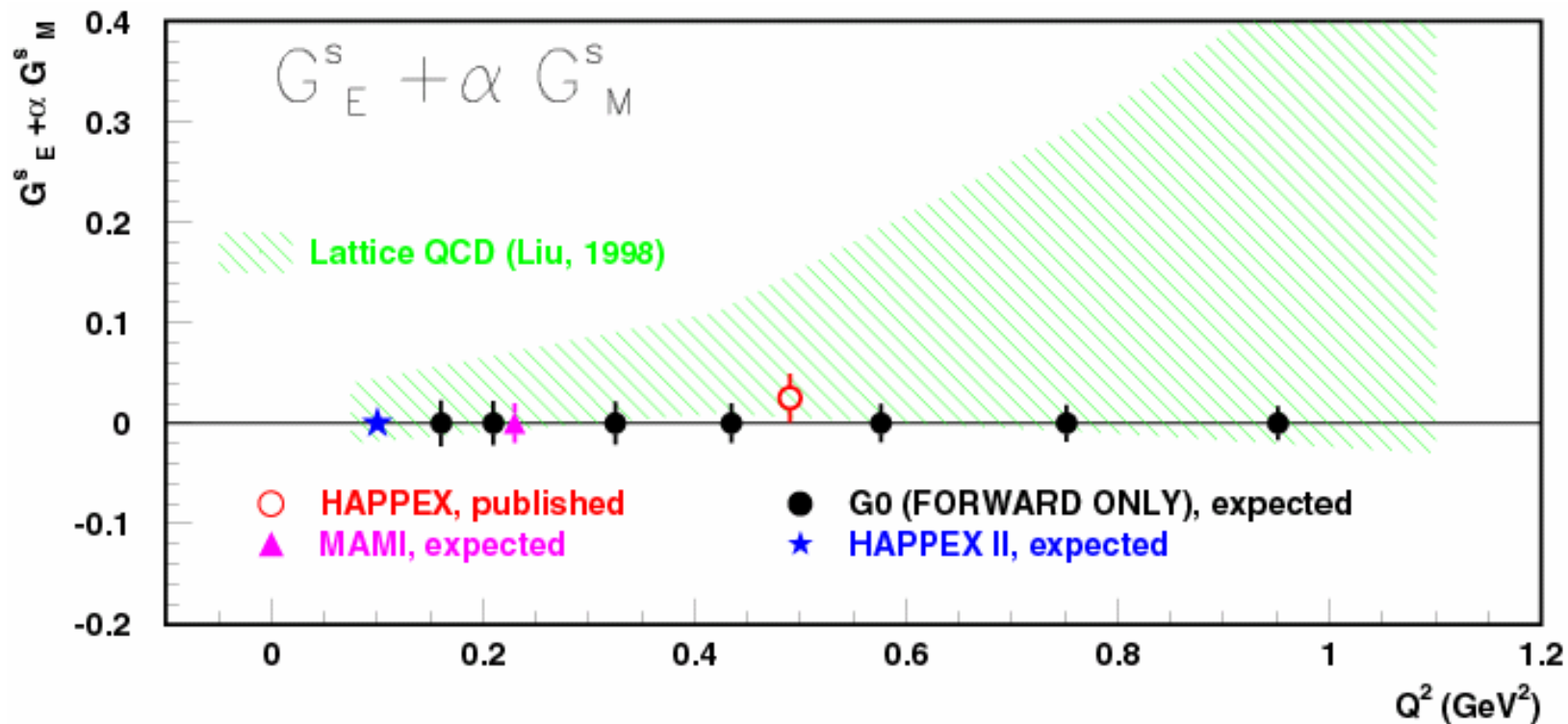
Strange Form Factors G_E^s and G_M^s



What we have on the books now

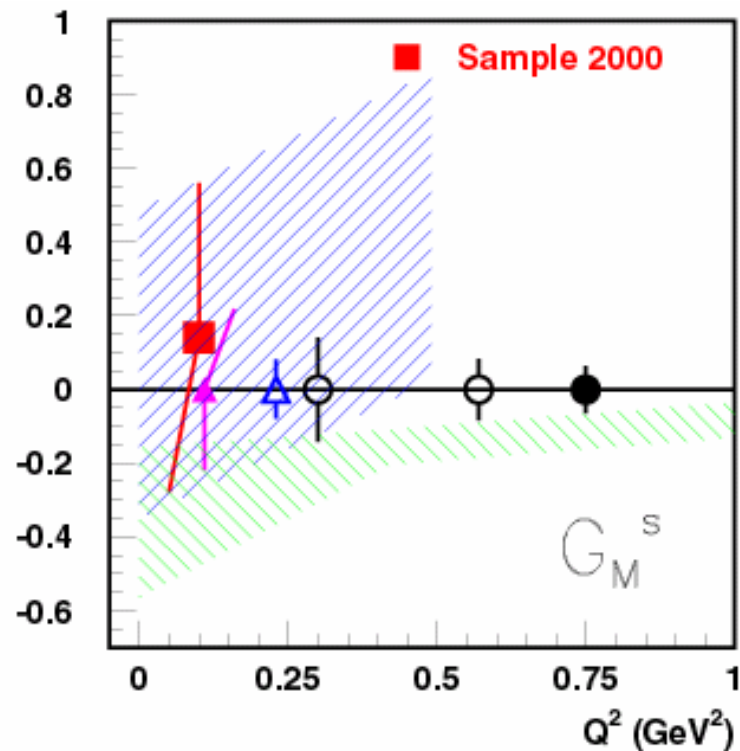
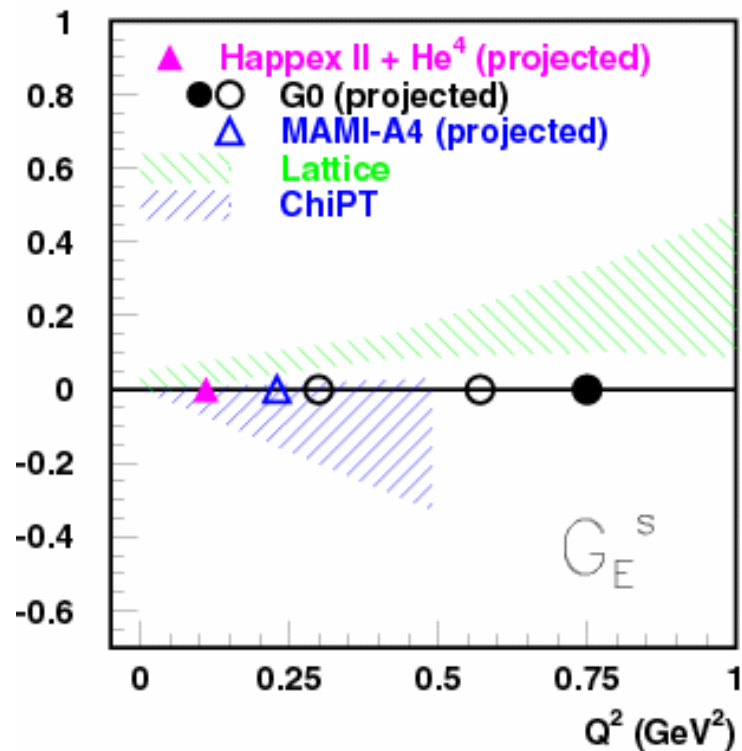
Strange Form Factors G_E^s and G_M^s

Expected Forward Angle Results by late 2003



Strange Form Factors G_E^s and G_M^s

Rosenbluth separation of G_E^s and G_M^s



Projected data indicated by open symbols are not approved yet

High Precision Nucleon Form Factors at JLab

Q^2 range

| | Present | Planned (12 GeV) | Comments |
|------------------------|---------|---------------------|--|
| G_E^p | 5.6 | 9.0 (14.0) | Precision Measurements Does G_E^p/G_M^p keep dropping linearly? |
| G_M^p | | (20.0) | $Q^2 > 14$ makes assumptions about G_E^p |
| G_E^n | 1.5 | 3.4 (5.5) | Precision Measurements ${}^3\vec{\text{He}}(\vec{e}, e' n)$ for $Q^2 > 1.5$ |
| G_M^n | 5.0 | (14.0) | Precision Measurements |
| $G_E^s + \alpha G_M^s$ | 0.5 | 1.0 | α small (non-0), now only at $Q^2=0.5$ |
| G_M^s | | 0.8 | Presently only approved at $Q^2=0.1$ and 0.8 |

Summary

- F^π First measurement away from $Q^2 \approx 0$
no Q^{-2} behavior yet
- G_E^p Precise data set up to $Q^2 = 5.6 \text{ (GeV/c)}^2$
charge differs from current distribution
 $Q^2 = 9 \text{ (GeV/c)}^2$ planned
- G_E^n 2 successful experiments, precise data anticipated
higher Q^2 possible and approved
- G_M^n $Q^2 < 1$ data from ${}^3\text{He}(e, e')$
high Q^2 data from ${}^2\text{H}(e, e'n)/{}^2\text{H}(e, e'p)$ anticipated
- G_E^s, G_M^s Happex-2, Happex-He, G0 coming up
+ Sample, Happex, Mainz
 \Rightarrow Stringent constraints on strangeness contributions
 \Rightarrow Enables Q-Weak Standard Model test